

Structure and properties of epitaxial perovskite $\text{Pb}(\text{Zr}_{0.52}\text{Ti}_{0.48})\text{O}_3/\text{La}_{0.7}\text{Sr}_{0.3}\text{MnO}_3$ heterostructures

Cheng Zou, Yuan-Fu Chen, Ping-Jian Li, Rui Fan, Bing Peng, Wen-Xu Zhang, Ze-Gao Wang, Xin Hao, Jing-Bo Liu, Wan-Li Zhang, Yan-Rong Li, and Run-Wei Li

Citation: *Journal of Applied Physics* **111**, 07D718 (2012); doi: 10.1063/1.3677866

View online: <http://dx.doi.org/10.1063/1.3677866>

View Table of Contents: <http://scitation.aip.org/content/aip/journal/jap/111/7?ver=pdfcov>

Published by the AIP Publishing

Articles you may be interested in

Thickness dependent functional properties of $\text{PbZr}_{0.52}\text{Ti}_{0.48}\text{O}_3/\text{La}_{0.67}\text{Sr}_{0.33}\text{MnO}_3$ heterostructures

J. Appl. Phys. **114**, 234103 (2013); 10.1063/1.4848017

Enhanced magnetoelectric effect in $\text{La}_{0.67}\text{Sr}_{0.33}\text{MnO}_3/\text{PbZr}_{0.52}\text{Ti}_{0.48}\text{O}_3$ multiferroic nanocomposite films with a SrRuO_3 buffer layer

J. Appl. Phys. **113**, 164106 (2013); 10.1063/1.4803057

Challenges in the stoichiometric growth of polycrystalline and epitaxial $\text{PbZr}_{0.52}\text{Ti}_{0.48}\text{O}_3/\text{La}_{0.7}\text{Sr}_{0.3}\text{MnO}_3$ multiferroic heterostructures using pulsed laser deposition

J. Appl. Phys. **112**, 064101 (2012); 10.1063/1.4751027

Role of dual-laser ablation in controlling the Pb depletion in epitaxial growth of $\text{Pb}(\text{Zr}_{0.52}\text{Ti}_{0.48})\text{O}_3$ thin films with enhanced surface quality and ferroelectric properties

J. Appl. Phys. **111**, 064102 (2012); 10.1063/1.3694035

Effect of oxygen stoichiometry on the ferroelectric property of epitaxial all-oxide $\text{La}_{0.7}\text{Sr}_{0.3}\text{MnO}_3/\text{Pb}(\text{Zr}_{0.52}\text{Ti}_{0.48})\text{O}_3$ thin-film capacitors

J. Vac. Sci. Technol. A **18**, 2412 (2000); 10.1116/1.1288195

The logo for AIP APL Photonics is displayed. It features the letters 'AIP' in a large, white, sans-serif font on the left, followed by a vertical line and the words 'APL Photonics' in a smaller, white, sans-serif font on the right. The background is a dark red with a bright yellow sunburst effect in the upper right corner.

APL Photonics is pleased to announce
Benjamin Eggleton as its Editor-in-Chief



Structure and properties of epitaxial perovskite $\text{Pb}(\text{Zr}_{0.52}\text{Ti}_{0.48})\text{O}_3/\text{La}_{0.7}\text{Sr}_{0.3}\text{MnO}_3$ heterostructures

Cheng Zou,^{1,2} Yuan-Fu Chen,^{1,a)} Ping-Jian Li,¹ Rui Fan,¹ Bing Peng,¹ Wen-Xu Zhang,¹ Ze-Gao Wang,¹ Xin Hao,¹ Jing-Bo Liu,¹ Wan-Li Zhang,¹ Yan-Rong Li,¹ and Run-Wei Li²

¹State Key Laboratory of Electronic Thin Films and Integrated Devices, University of Electronic Science and Technology of China, Chengdu 610054, People's Republic of China

²Key Laboratory of Magnetic Materials and Devices, Ningbo Institute of Material Technology and Engineering, Chinese Academy of Sciences, Ningbo 315201, People's Republic of China

(Presented 1 November 2011; received 7 October 2011; accepted 21 November 2011; published online 8 March 2012)

The morphology, crystalline structure of epitaxial heterostructures of $\text{Pb}(\text{Zr}_{0.52}\text{Ti}_{0.48})\text{O}_3/\text{La}_{0.7}\text{Sr}_{0.3}\text{MnO}_3$ (PZT/LSMO) grown on single crystalline SrTiO_3 substrates by pulse laser deposition (PLD), have been investigated. The morphology results show that the LSMO layers and PZT layers are smooth and homogenous. The crystalline structure measurements indicate that good epitaxial relationships between LSMO and PZT and STO were obtained. The effects of applied electric and magnetic fields on the physical properties of epitaxial perovskite ferroelectric/ferromagnetic heterostructures were investigated. The results show that the polarized electric field has a very significant influence on the transport properties of LSMO layers while has little influence on the magnetization, and the magnetic field has an obvious influence on the ferroelectric behavior of the PZT layer. © 2012 American Institute of Physics. [doi:10.1063/1.3677866]

INTRODUCTION

Recently, magnetoelectric effects (ME) are attracting much attention in multiferroic materials as either single phase¹ or as heterostructures.² In view of applications as well as basic research, epitaxial ferroelectric/ferromagnetic (FE/FM) heterostructures are interesting, since it has been shown that coupling between the magnetic and electric phases can offer control of the magnetic/electric responses under electric and magnetic field.^{3,4} Magnetoelectric coupling effect in multiferroic epitaxial heterostructures was first reported by Zheng *et al.*⁵ Due to the high remnant polarization, low coercive field, and high Curie temperature, perovskite $\text{PbZr}_x\text{Ti}_{1-x}\text{O}_3$ is a good ferroelectric candidate for the FE/FM heterostructures.⁶ Perovskite $\text{La}_x\text{Sr}_{1-x}\text{MnO}_3$ is another interesting candidate to fabricate perovskite FE/FM heterostructures because it is not only a ferromagnetic-layer element in the heterostructures but also as the bottom electrode for ferroelectric films. In addition, it has high Curie temperature and a close lattice constant and similar crystalline structure matching with perovskite ferroelectric $\text{PbZr}_x\text{Ti}_{1-x}\text{O}_3$. Moreover, $\text{La}_x\text{Sr}_{1-x}\text{MnO}_3$ is a half-metallic material and exhibits colossal magnetoresistance.⁷

There are some reports that the magnetoelectric effect of perovskite $\text{PbZr}_x\text{Ti}_{1-x}\text{O}_3/\text{La}_x\text{Sr}_{1-x}\text{MnO}_3$ heterostructures has been investigated. The ME voltage of epitaxial $\text{PbZr}_{0.3}\text{Ti}_{0.7}\text{O}_3$ on $\text{La}_{1.2}\text{Sr}_{1.8}\text{Mn}_2\text{O}_7$ single-crystal substrates is $\sim 87\%$ of the theoretical value predicted by a phenomenological thermodynamic model.⁸ Recently, a large change in magnetization was reported for the $\text{La}_{0.8}\text{Sr}_{0.2}\text{MnO}_3/\text{PbZr}_{0.2}\text{Ti}_{0.8}\text{O}_3$ bilayers in

response to polarization reversal.⁹ The interfacial strain effects in epitaxial multiferroic heterostructures of $\text{PbZr}_x\text{Ti}_{1-x}\text{O}_3/\text{La}_{0.7}\text{Sr}_{0.3}\text{MnO}_3$ have been investigated.¹⁰ However, the morphology and structure of epitaxial $\text{PbZr}_x\text{Ti}_{1-x}\text{O}_3/\text{La}_x\text{Sr}_{1-x}\text{MnO}_3$ heterostructures, and the effects of applied electric and magnetic fields on the physical properties of $\text{PbZr}_x\text{Ti}_{1-x}\text{O}_3/\text{La}_x\text{Sr}_{1-x}\text{MnO}_3$ heterostructures are still not systematically reported yet. Here, in this article, we focus on the morphology, structure, and the physical properties of $\text{Pb}(\text{Zr}_{0.52}\text{Ti}_{0.48})\text{O}_3/\text{La}_{0.7}\text{Sr}_{0.3}\text{MnO}_3$ (PZT/LSMO) heterostructures under applied electric and magnetic fields. The results show that the polarized electric field has a very significant influence on the transport properties of LSMO layers while has little influence on the magnetization, and the magnetic field has obvious influence on the ferroelectric behavior of the PZT layer.

EXPERIMENTAL

The epitaxial $\text{Pb}(\text{Zr}_{0.52}\text{Ti}_{0.48})\text{O}_3/\text{La}_{0.7}\text{Sr}_{0.3}\text{MnO}_3$ heterostructures were grown by pulse laser deposition. Firstly, 100-nm ferromagnetic LSMO was deposited on (001) SrTiO_3 substrates at a substrate temperature of 800 °C and an oxygen partial pressure of 0.4 mbar. Then, the LSMO film with a thickness of 100 nm was *ex situ* annealed for 1 h at 850 °C in air. Subsequently, 200-nm thick ferroelectric PZT film was deposited on LSMO film using a shadow mask. Finally, circular Cr/Au top metal electrodes with a diameter of 100 μm were e-beam evaporated on PZT by using a shadow mask. The morphology of the epitaxial layers was measured by atomic force microscopy (AFM), the magnetic domains and ferroelectric domains were characterized by magnetic force microscopy (MFM), and piezoelectric force microscopy (PFM), respectively. The crystalline structure

^{a)}Author to whom correspondence should be addressed. Electronic mail: yfchen@uestc.edu.cn.

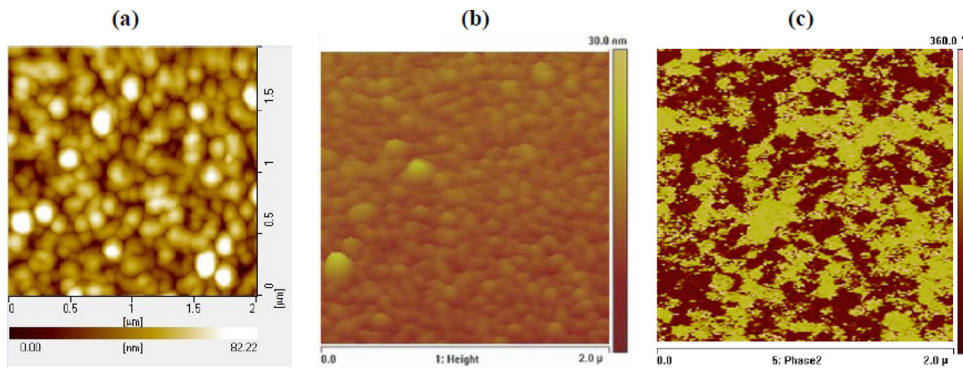


FIG. 1. (Color online) Surface morphology of the LSMO layer on the STO substrate (a). Surface morphology (b) and ferroelectric domain images (c) of PZT film on the LSMO/STO substrate.

was characterized by high-resolution x-ray diffraction (HRXRD). The transport properties of the PZT/LSMO heterostructures were performed by Keithley 2000, and Keithley 2400. The voltage source for PZT polarization was applied by Keithley 2400. The $P \sim E$ hysteretic loops were measured by a standard ferroelectric analyzer (Radiant Technologies, Precision LC) by using a conventional two-point technique with two Cr/Au metal electrodes on the PZT and LSMO layer, respectively. The magnetic property was performed by a VSM system at room temperature.

RESULTS AND DISCUSSION

The morphology of the LSMO layer deposited on STO were characterized by MFM, as shown in Fig. 1(a) respectively. From the morphology image shown in Fig. 1(a), one can find that the crystal grains of the LSMO layer are homogenous with an average size of 120 nm. The root-mean-square (RMS) roughness is 13.1 nm, which means the LSMO layer is high quality and very smooth.

The morphology and ferroelectric domains of the PZT layer deposited on the LSMO/STO substrate were characterized by PFM, as shown in Figs. 1(b), and 1(c), respectively. From Fig. 1(b), one can also observe that the crystal grains of the PZT layer are homogenous although the image is not so clear. From Fig. 1(c), one can observe that the ferroelectric domains are very clear and nice, which indicates the high quality of the PZT layer deposited on the LSMO/STO substrate.

In order to characterize the crystalline structure of PZT/LSMO heterostructures, HRXRD patterns of the $\theta-2\theta$ scan, and ω scan were measured, respectively. Fig. 2(a) presents

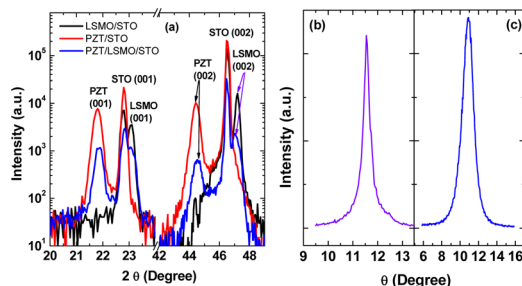


FIG. 2. (Color online) (a) $\theta-2\theta$ scan XRD pattern for a 30-nm-thick PZT film grown on 100 nm LSMO on the STO substrate. The omega-rocking curves of the LSMO (b) and (c) PZT films.

the $\theta-2\theta$ scan XRD pattern for a 200-nm thick PZT film grown on 100-nm-thick LSMO on the STO substrate. XRD results show that only the (00l) peaks are observed for both LSMO and PZT layers which are single crystalline and have an epitaxial relationship with Nb:SrTiO₃ substrates. Figs. 2(b) and 2(c) show the (001) omega-rocking curves of the LSMO and PZT films, respectively. The FWHM values of the (001) omega-rocking curve of the LSMO and PZT film were 0.349° and 1.428°, respectively, suggesting good epitaxial crystalline quality of LSMO and PZT layers.

The temperature dependence of the resistance of the LSMO layer is shown in the left top inset of Fig. 3(a). One can find that an obvious metal-insulator (or paramagnetic-ferromagnetic) transition occurs for the LSMO layer, and one can simply determine the metal-insulator transition temperature or ferromagnetic Curie temperature as high as 315 K by taking the maximal differential value. Sharp transition and high Curie temperature indicate that the epitaxial LSMO layer has high quality. In order to investigate the effect of polarized PZT on the transport properties of the underneath LSMO layer, the temperature dependence of resistance of the LSMO under various electric fields of 0, 0.4, and 0.8 V was measured, as shown in Fig. 3(a). One can find that the resistance change is strongly temperature dependent, as shown in the right bottom inset of Fig. 3(a). The resistance change is defined as $100 * [R_{(V, T)} - R_{(V=0, T)}] / R_{(V=0, T)}$, where $R_{(V, T)}$ is the resistance of LSMO at T K under an polarized voltage V applied between the LSMO (as bottom electrode) and the silver-paste electrode (as top electrode) and the LSMO under a polarized voltage of 0 V. One can find that even under a very small polarized voltage of 0.4 V, the maximal resistance change of LSMO at ~ 90 K is about 45.5%. When the polarized voltage reaches 0.8 V, it seems that the resistance change tends to be saturated. It is interesting that the minimal resistance change takes place at the Curie temperature of 315 K. For the $(R_V - R_0) / R_0 \sim T$ curve, the reason why the peak happens at 90-100 K, and the trough happens at Curie temperature is still unclear.

In order to investigate the effect of polarized electric field on the magnetic property of the LSMO layer, the room-temperature in-plane $M \sim H$ hysteretic loops under various polarized electric fields were performed. Figure 3(b) shows the PZT polarized electric field dependence of in-plane M-H hysteretic loops. One can find that under various applied

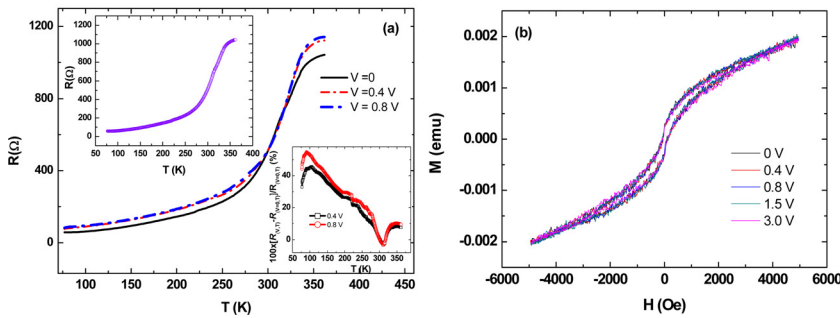


FIG. 3. (Color online) (a) Polarized electric field dependence of the transport property of the LSMO layer. The left top inset is the $R \sim T$ curve without polarization electric field and the right bottom inset is the $[R_{(V, T)} - R_{(V=0, T)}] / R_{(V=0, T)} \sim T$ curve. (b) Polarized electric field dependence of the magnetization hysteric loops of the LSMO layer.

electric fields of 0, 0.4, 0.8, 1.5, and 3 V, there is little change in the $M \sim H$ loops. Similar results have also observed for out-of-plane $M \sim H$ loops. This can be simply understood as follows. Firstly, the LSMO layer is sandwiched between the substrate and the PZT layer, which means that the substrate clamping effect will be dominant and the magnetoelectric effect will be limited. This is far different from that of $\text{La}_{0.8}\text{Sr}_{0.2}\text{MnO}_3/\text{PbZr}_{0.2}\text{Ti}_{0.8}\text{O}_3$ bilayers in Ref. 7, where LSMO is a freedom top layer and a large change in magnetization in response to polarization reversal was reported. Secondly, as shown in Fig. 3(a), the resistance change of LSMO is very small near around room temperature. This suggests that the property (including magnetization) of the LSMO layer is not so sensitive to the polarized electric field at room temperature. The magnetization of the LSMO layer might be more sensitive to the polarized electric field at low temperature around 90-100 K according to the right bottom inset of Fig. 3(a).

The effect of magnetic field on the ferroelectric properties of the PZT top layer was investigated. From the $R \sim T$ curve of LSMO shown in the left top inset of Fig. 3(a), the Curie temperature of LSMO is 315 K. So, the LSMO is ferromagnetic state at room temperature. From the $M \sim H$ curve of Fig. 3(b), one can find that the LSMO cannot be fully magnetized under 0.5 T. So, an in-plane magnetic field of 0.9 T was applied. Figure 4 shows the $P \sim E$ hysteretic loops with and without an in-plane magnetic field of 0.9 T. From Fig. 4, one can observe that an obvious increase in remnant and saturation polarization of PZT layer after a magnetic field of 0.9 T was applied. This obvious change in ferroelectric property of the PZT layer can be attributed to the change

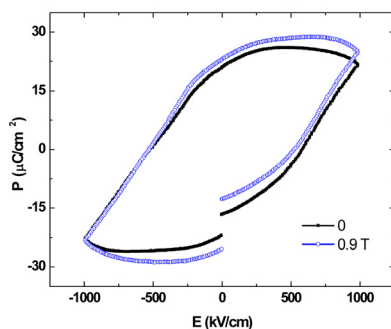


FIG. 4. (Color online) Magnetic field dependence of $P \sim E$ hysteretic loops of the PZT layer.

in the magnetized state of the underneath LSMO layer under an external magnetic field.

CONCLUSIONS

Epitaxial $\text{Pb}(\text{Zr}_{0.52}\text{Ti}_{0.48})\text{O}_3/\text{La}_{0.7}\text{Sr}_{0.3}\text{MnO}_3$ heterostructures were prepared on single crystalline SrTiO_3 substrates by pulse laser deposition (PLD). Morphology, crystalline structure, and the effects of electric and magnetic fields on the physical properties of $\text{Pb}(\text{Zr}_{0.52}\text{Ti}_{0.48})\text{O}_3/\text{La}_{0.7}\text{Sr}_{0.3}\text{MnO}_3$ heterostructures were investigated. The AFM morphology characterization shows that both the LSMO layer and PZT top layer are smooth and homogenous. The crystalline structure measurements indicate that good epitaxial relationships between LSMO and PZT and STO were obtained. The polarized electric field has very significant effect on the transport properties of LSMO layers while has little influence on the magnetization, and the magnetic field has an obvious influence on the ferroelectric behavior of the PZT layer.

ACKNOWLEDGMENTS

The authors acknowledge the financial support by the Major Program of the National Natural Science Foundation of China, National Natural Science Foundation of China, the Scientific Research Foundation for the Returned Overseas Chinese Scholars of the State Education Ministry of China, the Fundamental Research Funds for the Central Universities, the Youth Foundation of the University of Electronic Science and Technology of China (UESTC) and the start-up research project of UESTC.

¹N. Hur, S. Park, P. A. Sharma, J. S. Ahn, S. Guha, and S.-W. Cheong, *Nature* **429**, 392 (2004).

²W. Eerenstein, M. Wioral, J. L. Prieto, J. F. Scott, and N. D. Mathur, *Nature Mater.* **6**, 348 (2007).

³M. Fiebig, *J. Phys. D* **38**, R123 (2005).

⁴C.-W. Nan, M. I. Bichurin, S. Dong, D. Viehland, and G. Srinivasan, *J. Appl. Phys.* **103**, 031101 (2008).

⁵H. Zheng, J. Wang, S. E. Lofland, Z. Ma, L. Mohaddes-Ardabili, T. Zhao, L. Salamanca-Riba, S. R. Shinde, S. B. Ogale, and F. Bai, *Science* **303**, 661 (2004).

⁶J. F. Scott and C. A. Paz de Araujo, *Science* **246**, 1400 (1989).

⁷J. H. Park, E. Vescoso, H. J. Kim, C. Kwon, R. Ramesh, and T. Venkatesan, *Nature* **392**, 794 (1998).

⁸T. Wu, M. A. Zurbucher, S. Saha, R. V. Wang, S. K. Streiffer, and J. F. Mitchell, *Phys. Rev. B* **73**, 134416 (2006).

⁹I. Vrejoiu, M. Ziese, A. Setzer, P. D. Esquinazi, B. I. Birajdar, A. Lotnyk, M. Alexe, and D. Hesse, *Appl. Phys. Lett.* **92**, 152506 (2008).

¹⁰H. J. A. Molegraaf, J. Hoffman, C. A. F. Vaz, S. Gariglio, D. van der Marel, C. H. Ahn, and J.-M. Triscone, *Adv. Mater.* **21**, 3470 (2009).